Polymer Journal (2013) 45, 436–443

www.nature.com/pj

ORIGINAL ARTICLE

Crystallization of poly(ε-caprolactone) blocks confined in crystallized lamellar morphology of poly(ε-caprolactone)-*block*-polyethylene copolymers: effects of polyethylene crystallinity and confinement size

Takuya Sakurai, Hikaru Nagakura, Satoru Gondo and Shuichi Nojima

In poly(ε-caprolactone)-*block*-polyethylene (PCL-*b*-PE) diblock copolymers, the crystallizable temperature of PE blocks is sufficiently higher than that of PCL blocks, and accordingly, PE blocks crystallize first on quenching to form a crystallized lamellar morphology (PE lamellar morphology), followed by the crystallization of PCL blocks. We have investigated the crystallization behavior and crystal orientation of PCL blocks spatially confined in the PE lamellar morphology with different crystallinities of PE blocks χ_{PE} and layer thicknesses of PCL blocks d_{PCL} as a function of crystallization temperature $T_{c,PCL}$, where χ_{PE} and d_{PCL} are related to the rigidity and confinement size of the PE lamellar morphology, respectively. We found from differential scanning calorimetry results that the crystallization behavior of PCL blocks in PCL-*b*-PE with higher χ_{PE} and smaller d_{PCL} was significantly different from that in other PCL-*b*-PE copolymers. We also found using two-dimensional wide-angle X-ray diffraction that the orientation of PCL crystals changed moderately by changing $T_{c,PCL}$ in PCL-*b*-PE with higher χ_{PE} and smaller d_{PCL}, whereas it did not change substantially in PCL-*b*-PE with lower χ_{PE} or larger d_{PCL}. These results indicate that the rigidity and confinement size of the crystallized lamellar morphology, both of which can be controlled through the crystallization of the first blocks, are key factors for the crystallization of the second blocks in crystalline–crystalline diblocks with different crystallizable temperatures.
Polymer Journal (2013) **45,** 436–443; doi:10.1038/pj.2012.164; published online 12 September 2012

Keywords: crystalline–crystalline diblock copolymer; crystallization behavior; crystal orientation; lamellar morphology

INTRODUCTION

The morphology formation by the self-assembly of crystalline block copolymers has been extensively studied.[1–3] It is well known from these studies that such morphology formation depends on the relative values of three characteristic temperatures of crystalline block copolymers: the order–disorder transition temperature T_{ODT}, the crystallizable temperature of crystalline blocks T_c and the glass transition temperature of amorphous blocks T_g. When $T_{ODT} > T_g > T_c$, the microdomain structure is completely frozen by the vitrification of amorphous blocks before crystallization, and eventually constituent blocks crystallize within it (hard confinement).[4–10] When $T_{ODT} > T_c > T_g$, on the other hand, crystallization starts from the soft microdomain structure, and the resulting morphology depends on the segregation strength between two blocks; when it is sufficiently large, the crystallization is restricted in the microdomain (soft confinement),[11,12] whereas the microdomain structure is completely replaced with a crystallized lamellar morphology if the segregation strength is not sufficiently large.[13–15]

How crystalline blocks crystallize within lamellar morphologies with varying characteristics is interesting, and crystal orientation is one of the topics for confined crystallization in lamellar morphologies. Sun *et al.*,[16,17] for example, examined the crystal orientation of poly(ε-caprolactone) (PCL) blocks confined in vitrified lamellar microdomains of PCL-*block*-poly(4-vinylpyridine) (hard confinement) as a function of the layer thickness of PCL blocks (confinement size). They concluded that a parallel, perpendicular or random orientation with respect to the lamellar surface normal was formed with decreasing confinement size. Zhu *et al.*[18–20] also reported the crystal orientation of poly(ethylene oxide) (PEO) blocks in PEO-*block*-polystyrene (PEO-*b*-PS) as a function of crystallization temperature $T_{c,PEO}$. The crystal orientation changed drastically with increasing $T_{c,PEO}$ from random to perpendicular and finally to parallel in

Department of Organic and Polymeric Materials, Graduate School of Science and Engineering, Tokyo Institute of Technology, Tokyo, Japan
Correspondence: Professor S Nojima, Department of Organic and Polymeric Materials, Graduate School of Science and Engineering, Tokyo Institute of Technology, H-125, 2-12-1 Ookayama Meguro-Ku, Tokyo 152-8552, Japan.
E-mail: snojima@polymer.titech.ac.jp
Received 7 June 2012; revised 20 July 2012; accepted 23 July 2012; published online 12 September 2012

relation to the lamellar surface normal. Ho *et al.*[21] reported on the crystal orientation of poly(L-lactide) (PLLA) blocks confined in the lamellar morphology of PLLA-*b*-PS (soft confinement) and concluded that the c-axis of PLLA crystals is always perpendicular to the lamellar surface, although the interface of lamellar microdomains undulated with crystallization.

We have recently investigated the crystallization behavior and crystal orientation of PCL blocks in PCL-*block*-polyethylene (PCL-*b*-PE) diblock copolymers,[22–26] where PE blocks crystallized first upon quenching to form a crystallized lamellar morphology (PE lamellar morphology), and subsequently, PCL blocks crystallized in this morphology. Because the PE lamellar morphology consists of hard lamellar crystals covered with soft PE amorphous layers, the spatial confinement of the PE lamellar morphology is expected to be intermediate between hard and soft against the crystallization of PCL blocks. We reported, for example, that the orientation of PCL crystals changed significantly on changing the PCL layer thickness d_{PCL} in the PE lamellar morphology with a fixed crystallinity of PE blocks χ_{PE} ($\sim$23%).[25] That is, the c-axis of the PCL blocks was always parallel to the PE lamellar surface normal at large d_{PCL} (16.5 nm $> d_{PCL} >$ 10.7 nm), whereas the orientation of PCL crystals depended moderately on the crystallization temperature of PCL blocks $T_{c,PCL}$ at smaller d_{PCL} ($\sim$8.8 nm). We concluded that the PE lamellar morphology with χ_{PE} $\sim$23% played a similar role to glassy lamellar microdomains regarding spatial confinement against the crystal orientation of PCL blocks.

In this study, we examined the crystallization behavior and crystal orientation of PCL blocks confined in the PE lamellar morphology formed in PCL-*b*-PE copolymers with reduced χ_{PE} as well as different d_{PCL}. This is because the decrease in χ_{PE} might change the rigidity of the PE lamellar morphology, that is, confinement nature (hard or soft), to yield a substantial difference in the crystallization behavior and crystal orientation of the PCL blocks, as mentioned above. For this purpose, we synthesized several PCL-*b*-PE copolymers with different amounts of ethyl branches in the PE blocks to vary the χ_{PE}. We elucidated the combined effects of χ_{PE} and d_{PCL} on the subsequent crystallization of PCL blocks.

EXPERIMENTAL PROCEDURE

Samples and sample preparation

The samples used in this study were double crystalline PCL-*b*-PE diblock copolymers, which were obtained by the hydrogenation of PCL-*block*-polybutadiene (PCL-*b*-PB) anionically synthesized. Detailed methods for the synthesis of PCL-*b*-PB were described in our previous works.[22,23] We also synthesized PCL-*b*-PE copolymers with more ethyl branches in PE blocks to decrease χ_{PE}. The method used to synthesize such copolymers is briefly described. First, butadiene monomers in toluene with a small amount of 1,2-dipiperidinoethane, which increases the 1,2-addition of butadiene monomers,[27,28] were polymerized at room temperature using *n*-butyllithium as an initiator, followed by the addition of ε-caprolactone monomers to synthesize PCL-*b*-polybutadiene at 0 °C. The PCL-*b*-PB copolymers thus synthesized were finally hydrogenated to obtain PCL-*b*-PE.

The molecular characteristics of the samples are described in Table 1, where we divide the samples into two groups according to d_{PCL}. Group A consists of E07 and E23 with small d_{PCL} (8.3–8.8 nm) but different χ_{PE}, whereas group B consists of E16 and E24 with larger d_{PCL} (10.4–10.7 nm). Here, E23 and E24 are identical to CL33 and CL38, respectively, used in our previous study.[25] The volume fraction of each block in PCL-*b*-PE was calculated from the mole fraction derived by ^{1}H-NMR and the specific volume of each block; for amorphous PE[29]

$$v_{sp}(T) = 1.1696 + (1.77 \times 10^{-4}) \times T$$

and for amorphous PCL[30]

$$v_{sp}(T) = 0.9106 + (6.01 \times 10^{-4}) \times T,$$

where $v_{sp}(T)$ is in cm^3 g^{-1} and T in °C.

Differential scanning calorimetry measurements

A PerkinElmer Pyris 1 calorimeter was used at a heating rate of 10 °C min^{-1} over a temperature range between 0 and 120 °C to evaluate the melting temperature and crystallinity of both blocks. The crystallinity was calculated from the endothermic peak area during heating, assuming that the heat of fusion for perfect PCL and PE crystals was 135[30] and 277 J g^{-1},[29] respectively. In addition, the isothermal crystallization behavior of PCL blocks in the PE lamellar morphology was examined as a function of crystallization time t using differential scanning calorimetry.

One-dimensional small-angle X-ray scattering measurements

The microdomain structure and crystallized lamellar morphology of the samples were investigated using one-dimensional small-angle X-ray scattering (SAXS) with synchrotron radiation, which was performed at the Photon Factory in High Energy Accelerator Research Organization, Tsukuba, Japan, with a small-angle X-ray equipment installed at the BL-10C beam line. The detector was an one-dimensional position-sensitive proportional counter with an effective length of 20 cm, with which isotropic scattering was obtained as a function of wave number s ($= (2/\lambda)\sin\theta$, λ: X-ray wavelength ($= 0.1488$ nm) and 2θ: scattering angle). Details of the equipment and instrumentation have already been described.[31] The long period of the microdomain structure and crystallized lamellar morphology was evaluated from the primary peak position of one-dimensional SAXS curves after correcting for background scattering. The method for evaluating d_{PCL} has previously been described.[25]

Table 1 Molecular characteristics of PCL-*b*-PE copolymers used in this study

Group	*Sample code*	*Total* M_n[a]	M_w/M_n[a]	*PCL:PE*[b] *(vol%)*	*Mol % of 1–2 linkage*[b]	$T_{m,PCL}$[c] *(°C)*	$T_{m,PE}$[d] *(°C)*	χ_{PE}[e] *(%)*	d_{PCL}[f] *(nm)*
A	E07	14 100	1.02	34:66	15.3	54	85	7	8.3
	E23[g]	13 700	1.05	33:67	9.7	51	101	23	8.8
B	E16	14 800	1.07	37:63	12.0	54	93	16	10.4
	E24[g]	13 800	1.12	38:62	9.7	54	101	24	10.7

Abbreviations: DSC, differential scanning calorimetry; PCL, poly(ε-caprolactone); PE, polyethylene.
[a]Determined by gel permeation chromatography using polystyrene as a standard.
[b]Determined by ^{1}H-NMR.
[c]Melting temperature of PCL blocks determined by DSC during heating at 10 °C min^{-1}.
[d]Melting temperature of PE blocks determined by DSC during heating at 10 °C min^{-1}.
[e]Crystallinity of PE blocks determined by DSC assuming that the heat of fusion for perfect PE crystals is 277 J g^{-1},[29].
[f]Layer thickness of PCL blocks calculated from the long period evaluated from one-dimensional small-angle X-ray scattering and the volume fraction of PE and PCL blocks by considering the crystallinity of PE blocks.
[g]E23 and E24 are identical to CL33 and CL38, respectively, in our previous study,[25] but DSC measurements were performed again to obtain $T_{m,PCL}$, $T_{m,PE}$ and χ_{PE}.

Two-dimensional SAXS and wide-angle X-ray diffraction measurements

First, the PE lamellar morphology was uniaxially oriented to investigate the internal crystal orientation of PCL blocks. Detailed methods for the orientation are described in our previous publication.[25] The uniaxial orientation of the PE lamellar morphology was verified using two-dimensional SAXS, and the crystal orientation of PCL blocks in the oriented PE lamellar morphology was examined by two-dimensional wide-angle X-ray diffraction (2D-WAXD), both using a Nanoviewer (Rigaku, Tokyo, Japan) with a rotating anode X-ray generator operating at 45 kV and 60 mA. The wavelength used was 0.1542 nm (Cu Kα line). The detector for both measurements was an image plate (BAS-SR 127, FUJI Film, Tokyo, Japan) with an effective size of $12.7 \times 12.7\,cm^2$, and the accumulation time was 1 h. We finally evaluated the degree of crystal orientation from azimuthal plots for (110) and (200) diffraction intensities arising from the PCL crystals.[32]

RESULTS AND DISCUSSION

Crystallization of PCL-*b*-PE copolymers

Figure 1 shows differential scanning calorimetry melting curves during heating at $10\,^{\circ}C\,min^{-1}$ for the samples gradually cooled from 120°C (both blocks are amorphous) to 0 °C (both blocks crystallized), where we find two endothermic peaks: a sharp peak located at ~55 °C and a diffuse peak at 85–100 °C (indicated by arrows). The melting temperature of the PCL and PE homopolymers[29,30] indicates that the former peak corresponds to PCL melting with the latter corresponding to PE melting. Because the two endothermic peaks are adequately separated, we can expect that the crystallization of PCL blocks starts after PE blocks crystallize completely when the sample is quenched from the microphase-separated melt to low temperatures.

Figure 2 shows the one-dimensional SAXS curves of each sample at the temperatures indicated. We find a series of scattering peaks at 120 °C, the positions of which exactly correspond to a ratio of $1:2:7^{1/2}$: 4 for group A (E07 and E23) and 1:2:3:4 for group B (E16 and E24), indicating that a cylindrical microdomain structure is formed in the melt for group A and a lamellar microdomain structure for group B. When only PE blocks crystallize at 70 °C, the higher-order peaks disappear and the primary and secondary peaks become diffuse and shift appreciably to lower angles, suggesting that the both cylindrical and lamellar microdomain structures are completely replaced with the PE lamellar morphology, an alternating structure consisting of thin lamellar crystals and amorphous layers, by the crystallization of PE blocks. This morphological transition observed in PCL-*b*-PE with the crystallization of PE blocks has been previously reported.[22,23] The PCL blocks crystallize after being quenched further to 25 °C, but the SAXS curve is similar to that observed at 70 °C, suggesting that the crystallization of PCL blocks occurs in the existing PE lamellar morphology without further morphological transition. Therefore, it is possible to investigate the crystallization behavior and crystal orientation of PCL blocks in various PE lamellar morphologies with different χ_{PE} and d_{PCL}. We evaluated the d_{PCL} of each sample from the primary peak position of the SAXS curves at 70 °C and found that d_{PCL} remained nearly constant in group A, although E07 had a significantly lower χ_{PE} than E23 (Table 1). Similarly, E16 had a lower χ_{PE} than E24, with a similar d_{PCL} (group B).

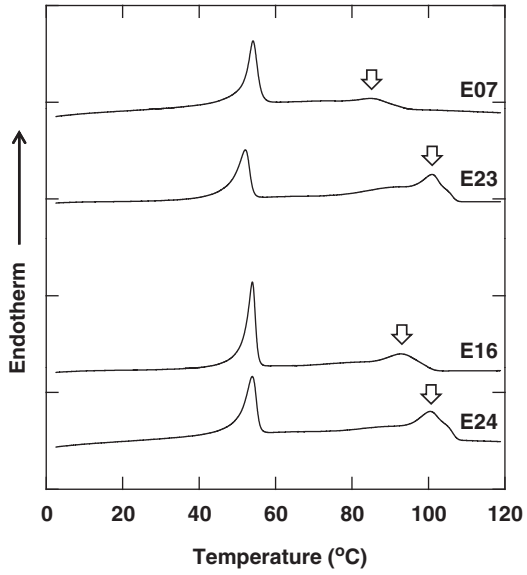

Figure 1 Differential scanning calorimetry curves obtained during heating at $10\,^{\circ}C\,min^{-1}$ for each sample. Upper two curves belong to group A and lower two curves to group B. The arrows indicate the melting of polyethylene blocks.

Figure 3 shows the long period, evaluated from the primary peak position of SAXS curves, plotted against temperature T for all samples. The microdomain structure is formed at temperatures above $T_{m,PE}$ ($\geqslant 100\,^{\circ}C$), where the long period increases gradually with decreasing T due to several factors such as the change in block incompatibility and chain conformation.[33] The PE blocks crystallize promptly with further decreasing T ($80\,^{\circ}C \geqslant T \geqslant 60\,^{\circ}C$). The long period at $T \geqslant 100$°C extrapolated to lower temperatures ($80\,^{\circ}C \geqslant T \geqslant 60\,^{\circ}C$) (indicated by thick broken lines for E23 and thin lines for E24) is significantly smaller than the actual long period at $80\,^{\circ}C \geqslant T \geqslant 60\,^{\circ}C$ (represented by an arrow in Figure 3), indicating again that PE blocks crystallize to form the PE lamellar morphology by destroying existing lamellar microdomain structures. The PCL blocks finally crystallize at temperatures below 45 °C, at which the long period does not change drastically. A faint change in the long period observed at $T \geqslant 30\,^{\circ}C$ in Figure 3 might be ascribed to the distortion of the PE lamellar morphology, as discussed in our previous studies.[22,23]

Crystallization behavior of PCL blocks

Figure 4 shows the time evolution of the crystallinity of PCL blocks $\chi_{PCL}(t)$ isothermally crystallized at 35 °C, where samples have been quenched from the melt to 70 °C to crystallize PE blocks first, followed by further quenching to 35 °C to crystallize PCL blocks. The time dependence of $\chi_{PCL}(t)$ shows a sigmoidal evolution for E07, E16 and E24, suggesting that the crystallization behavior of the PCL blocks is similar to that of general homopolymers without spatial confinement. However, we find that the crystallization of E23 is an extremely slow process that is substantially different from that of the other polymers. It should be noted that the crystallization rate at lower temperatures (for example, 0 °C) was too fast and that at higher temperatures (45 °C) was too slow to be pursued using differential scanning calorimetry. Therefore, the time evolution of $\chi_{PCL}(t)$ could only be obtained over a limited temperature range.

We applied Avrami analysis[34,35] for the time evolution of $\chi_{PCL}(t)$ to evaluate the Avrami index n as well as the half-time of crystallization $\tau_{1/2}$. The value of n provides information on the nucleation and crystal growth of confined blocks,[36,37] and $\tau_{1/2}$ is a measure of the crystallization rate of PCL blocks. Table 2 shows n and $\tau_{1/2}$, together with the orientation mode of PCL crystals (obtained later). We find that n and $\tau_{1/2}$ of E23 are distinctly different from the values gathered from other copolymers. That is, n is significantly small and $\tau_{1/2}$ is extremely large, suggesting that the effective spatial confinement in

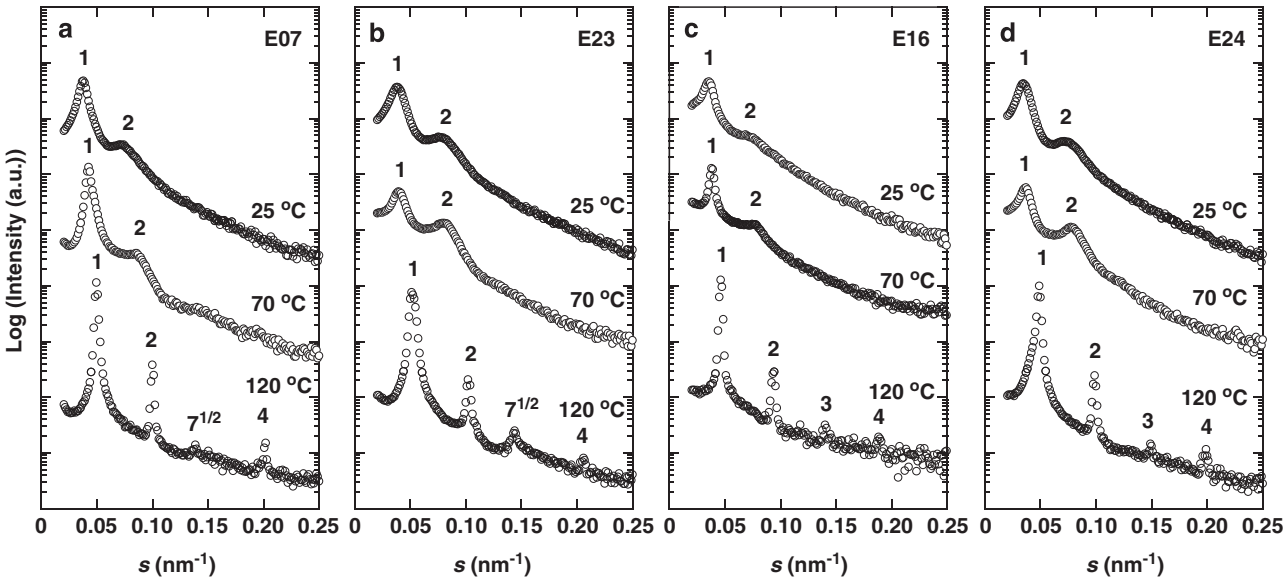

Figure 2 One-dimensional small-angle X-ray scattering (SAXS) curves of E07 (**a**), E23 (**b**), E16 (**c**) and E24 (**d**) measured at 120 °C (bottom), 70 °C (middle) and 25 °C (top). The SAXS curves at 70 and 25 °C are successively shifted upward for legibility.

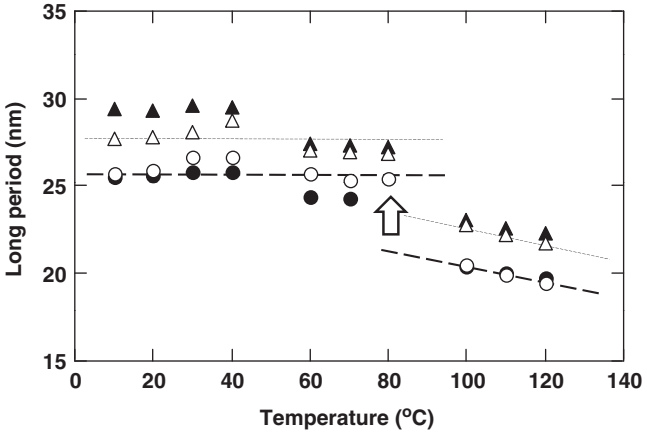

Figure 3 Long period plotted against temperature for E07 (●), E23 (○), E16(▲) and E24 (△). The thick broken line is a guide for E23 and the thin broken line for E24. The arrow indicates the discontinuous increase in the long period in E23 due to the crystallization of polyethylene blocks.

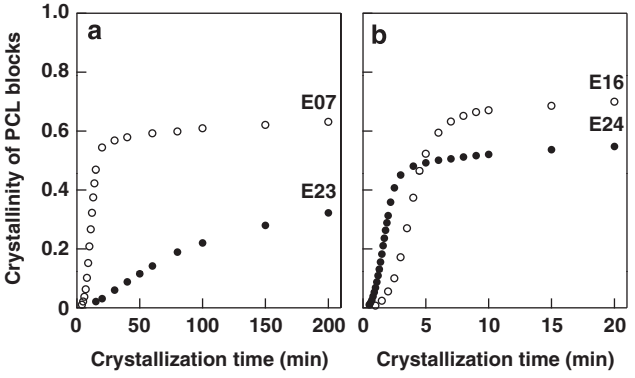

Figure 4 The crystallinity of poly(ε-caprolactone) (PCL) blocks for group A (**a**) and group B (**b**) plotted against crystallization time during isothermal crystallization at 35 °C.

Table 2 Avrami index *n* and half-time of crystallization $\tau_{1/2}$ for PCL blocks crystallized at $T_{c,PCL} = 35$ °C

Group	*Sample code*	n	$\tau_{1/2}$ *(min)*	*c-axis of PCL crystals in relation to PE lamellar surface normal*
A	E07	3.4	12.0	Parallel
	E23	1.5	112.5	Perpendicular
B	E16	3.1	4.2	Parallel
	E24	2.8	2.1	Parallel

Abbreviations: PCL, poly(ε-caprolactone); PE, polyethylene.

E23 is unique. E23 has a small d_{PCL} and high χ_{PE} such that we can easily suppose that its PE lamellar morphology is rigid, which will effectively confine PCL blocks, thereby yielding a difference in the crystallization behavior and eventually crystal orientation of PCL blocks, as described in section 'Crystal orientation of PCL blocks confined in oriented PE lamellar morphology'. It should be noted that n depended significantly on $T_{c,PCL}$ in our previous study for PCL-*b*-PE copolymers with small d_{PCL} and high χ_{PE}[23]; n was ~3.0 at higher $T_{c,PCL}$ (>42 °C) but was ~1.6 at lower $T_{c,PCL}$ (<40 °C). This fact suggests that the stability (or rigidity) of the PE lamellar morphology may be intimately related to $T_{c,PCL}$ for all PCL-*b*-PE copolymers. Ho *et al.*[21] observed that the effective confinement allowed for a change in the nucleation mechanism to yield different crystal orientations in crystalline-amorphous diblock copolymers, which will also be explained in terms of the stability of existing lamellar morphologies against subsequent crystallization.

In summary, the combined effects of χ_{PE} and d_{PCL} control the crystallization behavior of PCL blocks confined in the PE lamellar morphology. That is, the rigidity of the confinement space (χ_{PE}) and the confinement size (d_{PCL}) are key factors to understand the crystallization behavior of PCL blocks spatially confined in the PE lamellar morphology.

Orientation of PE lamellar morphology

We applied rotational shear to the samples for the uniaxial orientation of the PE lamellar morphology to examine the crystal orientation of PCL blocks confined in the PE lamellar morphology. Figure 5 shows 2D-SAXS patterns viewed from the Y direction for all samples at 70 °C (where only PE blocks crystallized) and 45 °C (both blocks crystallized), where X represents the shear direction and Y is perpendicular to the shear direction (see illustration in Figure 5). We find a couple of diffraction spots on the meridian in all samples investigated. We obtained similar 2D-SAXS patterns when viewed from the X direction but no diffraction from the Z direction at both temperatures (see Figure 3 in Higa *et al*.[25] These results clearly indicate that the PE lamellar morphology preferentially orients parallel to the shear direction; furthermore, this orientation is completely preserved after the crystallization of PCL blocks at lower temperatures. Therefore, it is possible to crystallize PCL blocks within the uniaxially oriented PE lamellar morphology and examine the crystal orientation of PCL blocks. It should be noted that the long period evaluated from the diffraction spots shown in Figure 5 exactly corresponds to that derived from isotropic samples (Figure 3), which means that rotational shear does not substantially alter the PE lamellar morphology.

Crystal orientation of PCL blocks confined in oriented PE lamellar morphology

Two-dimensional WAXD measurements were performed to examine the crystal orientation of PCL blocks confined in the PE lamellar morphology. Figure 6 shows the 2D-WAXD patterns viewed from the Y direction for each sample isothermally crystallized at 0 and 45 °C. The 2D-WAXD patterns of PCL-*b*-PE measured at 70 °C were demonstrated in our previous report,[25] where only PE blocks crystallized and we found two major diffractions arising from the (110) and (200) planes of PE crystals. The WAXD patterns shown in Figure 6 consist of the combined diffractions from PE and PCL crystals, where the diffraction angles 2θ from the (110) and (200) planes of PE crystals are almost identical to those of PCL crystals. Therefore, we subtracted the diffraction intensities of PE crystals from the total 2D-WAXD intensities and then azimuthally averaged the (110) and (200) diffraction intensities from PCL crystals. The details of this process have been previously described.[25]

Figures 7 and 8 show the WAXD intensities from the (110) and (200) planes of PCL crystals plotted against azimuthal angle φ for each sample crystallized at $T_{c,PCL} = 0$ °C (left) and 45 °C (right), where $\varphi = 0^\circ$ and $\varphi = 180^\circ$ correspond to the meridian. At lower temperatures (for example, 0 °C), the (110) and (200) diffraction curves from E07, E16 and E24 have two distinct peaks at $\varphi \sim 90^\circ$ and 270°, and those from E23 seem to have no peak or faint peaks at $\varphi \sim 90^\circ$ and 270°. These results are observed at $0\ ^\circ\text{C} \leqslant T_{c,PCL} \leqslant 20\ ^\circ\text{C}$. At higher temperatures (45 °C), E23 has four (110) diffraction peaks at $\varphi \sim 65^\circ$, 115°, 245° and 295° and two (200) diffraction peaks at $\varphi \sim 0^\circ$ and 180°, although the (110) and (200) diffraction curves of E07, E16 and E24 still have two peaks similar to those at lower temperatures. These results are also observed at $25\ ^\circ\text{C} \leqslant T_{c,PCL} \leqslant 45\ ^\circ\text{C}$. Figures 7 and 8 indicate that the crystal orientation of PCL blocks in E23 depends significantly on $T_{c,PCL}$; that is, the c-axis of PCL crystals is almost random at $0\ ^\circ\text{C} \leqslant T_{c,PCL} \leqslant 20\ ^\circ\text{C}$, whereas it is perpendicular to the PE lamellar surface normal at $25\ ^\circ\text{C} \leqslant T_{c,PCL} \leqslant 45\ ^\circ\text{C}$. The c-axis of PCL crystals in E07, E16 and E24 is, however, parallel to the PE lamellar surface normal irrespective of $T_{c,PCL}$. It is clear from Table 2 that the difference in crystal orientation between E23 and other PCL-*b*-PE copolymers is intimately related to the difference in crystallization behavior.

Figure 9 shows the crystal orientation of PCL blocks confined in the PE lamellar morphology with different χ_{PE} and d_{PCL}. Although it

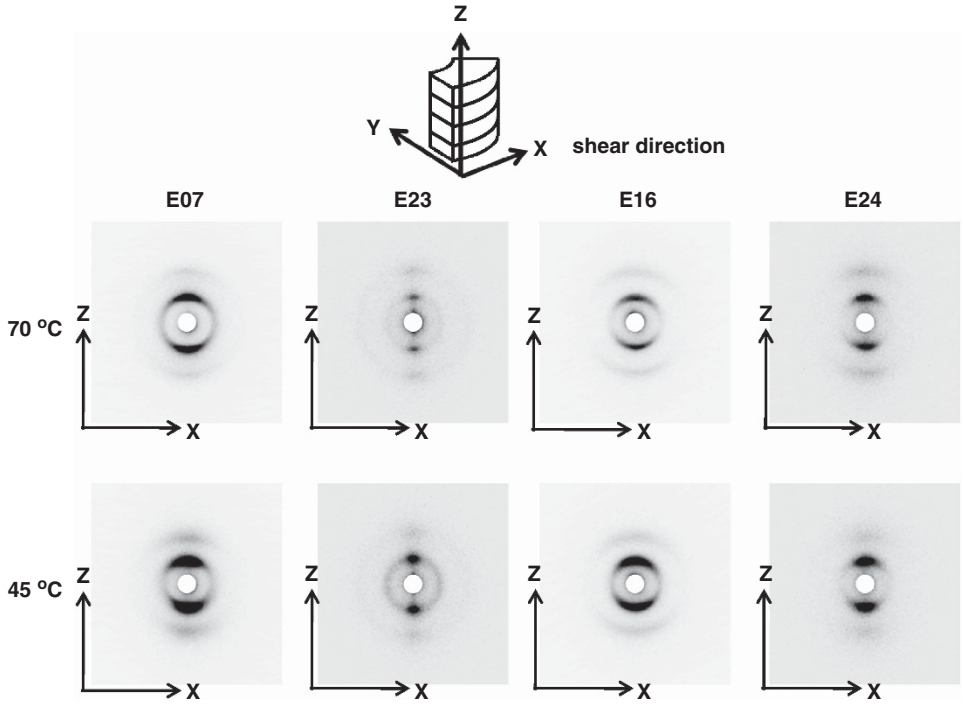

Figure 5 Two-dimensional small-angle X-ray scattering patterns of uniaxially oriented E07, E23, E16 and E24 measured at 70 °C (upper panels) and 45 °C (lower panels) when viewed from the Y direction, which is perpendicular to the shear direction, as shown in the illustration (top).

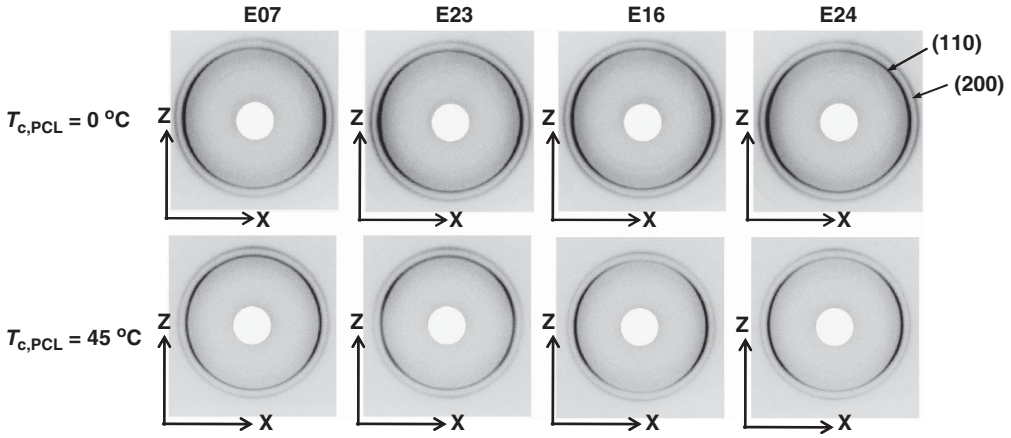

Figure 6 Two-dimensional wide-angle X-ray diffraction patterns of E07, E23, E16 and E24 crystallized at 0 °C (upper panels) and 45 °C (lower panels) when viewed from the Y direction. PCL, poly(ε-caprolactone).

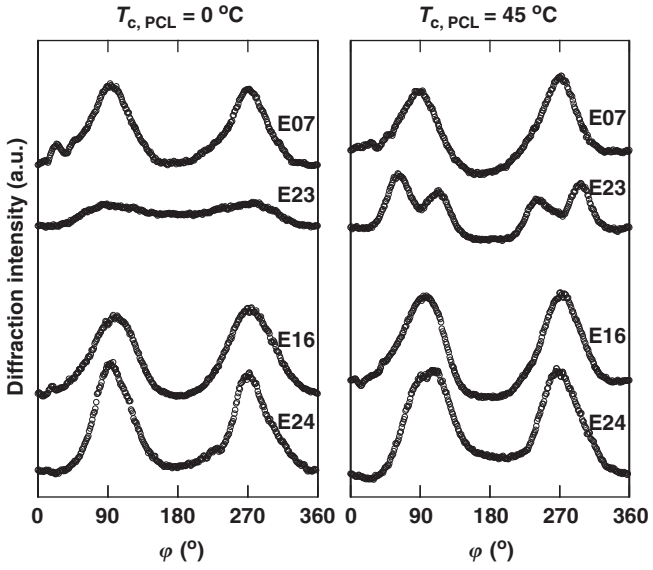

Figure 7 The diffraction intensity from the (110) plane of PCL crystals plotted against azimuthal angle φ at $T_{c,PCL} = 0\,^{\circ}C$ (left) and $T_{c,PCL} = 45\,^{\circ}C$ (right). $\varphi = 0^{\circ}$ and 180° correspond to the meridian. The data for E23 were reported in our previous study.[25] a.u., arbitrary unit; PCL, poly(ε-caprolactone).

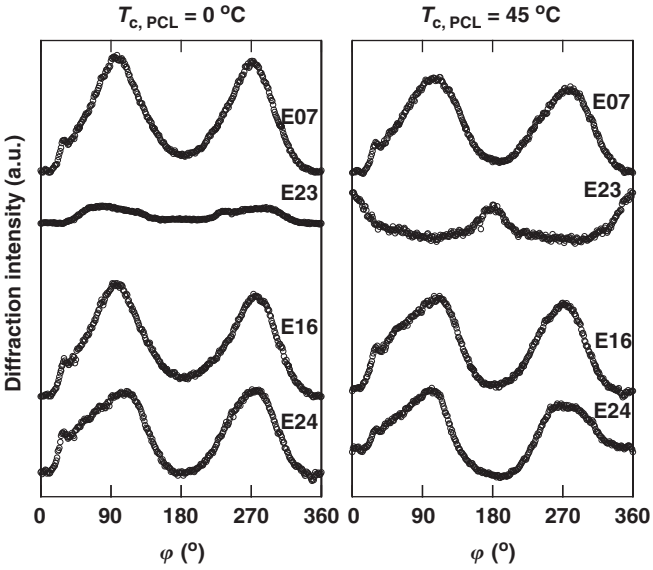

Figure 8 The diffraction intensity from the (200) plane of PCL crystals plotted against azimuthal angle φ at $T_{c,PCL} = 0\,^{\circ}C$ (left) and $T_{c,PCL} = 45\,^{\circ}C$ (right). a.u., arbitrary unit; PCL, poly(ε-caprolactone).

is difficult to evaluate actual PCL crystallite sizes spatially confined in the PE lamellar morphology, they are speculated to be moderately smaller than the confinement size (that is, 8.3–10.7 nm) considering the crystallite sizes formed in PCL thin films.[38]

Group A (E07 and E23) has smaller and similar d_{PCL} (8.3–8.8 nm), but χ_{PE} is extremely different between the E07 and E23, resulting in a difference in the rigidity of the confined space, which substantially controls the orientation of PCL crystals; at $0\,^{\circ}C \leqslant T_{c,PCL} \leqslant 20\,^{\circ}C$, the c-axis of PCL crystals in E23 is random but perpendicular against the lamellar surface normal at $25\,^{\circ}C \leqslant T_{c,PCL} \leqslant 45\,^{\circ}C$, whereas that in E07 is parallel irrespective of $T_{c,PCL}$. Group B (E16 and E24) has larger d_{PCL} (10.4–10.7 nm) with different χ_{PE}, where the c-axis of PCL crystals is parallel to the lamellar surface normal irrespective of $T_{c,PCL}$. It has been reported that when the confinement size is sufficiently large the c-axis is always parallel to the lamellar surface normal, even in soft or glassy lamellar morphologies, which is consistent with our results.

By considering the $T_{c,PCL}$ dependence of crystal orientation in E23 and E24, we have already concluded that the PE lamellar morphology with higher χ_{PE} (23–24%) has a similar role to glassy lamellar microdomains regarding spatial confinement against subsequent PCL crystallization (hard confinement).[25] That is, our results for the crystal orientation of PCL blocks in E23 and E24 qualitatively agree with those of block chains in glassy lamellar microdomain structures reported by Sun *et al.*[16,17] for PCL-*block*-poly(4-vinylpyridine) and by Zhu *et al.*[18–20] for PEO-*block*-polystyrene. For example, Sun *et al.* showed that the crystallization mechanism of PCL blocks changed from homogeneous to heterogeneous nucleation with increasing d_{PCL} to yield a situation in which the c-axis of PCL crystals changed from being randomly oriented to being parallel to the lamellar surface

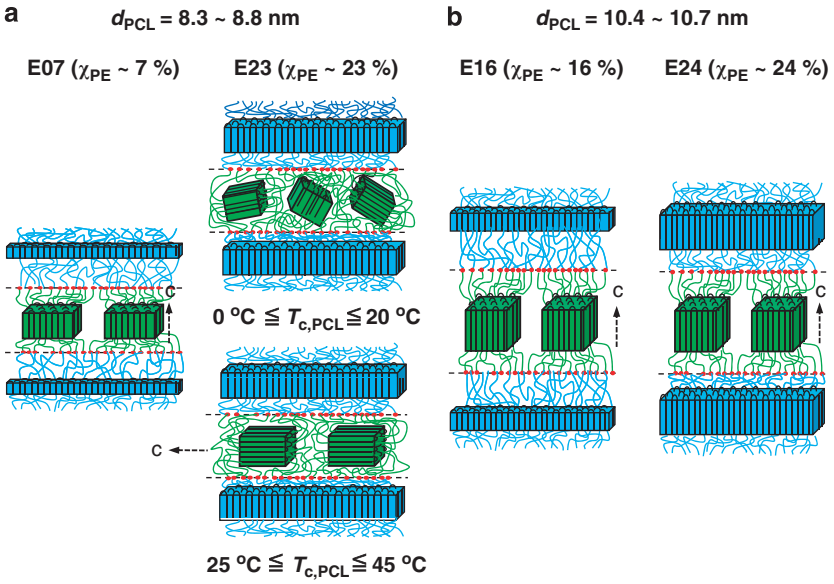

Figure 9 Schematic illustration showing the crystal orientation of PCL blocks spatially confined in the polyethylene lamellar morphology for group A (**a**) and group B (**b**). The crystal orientation of PCL blocks in E07, E16 and E24 is independent of $T_{c,PCL}$. PCL, poly(ε-caprolactone).

normal. The perpendicular orientation of PCL crystals was also observed only for the lamellar microdomain structure with intermediate d_{PCL}.

The PE lamellar morphology formed in E07 has a smaller d_{PCL} comparable with E23, but we observed an extremely different crystal orientation similar to that observed in E16 and E24 with larger d_{PCL} (10.4–10.7 nm). This fact suggests that the effect of narrower spatial confinement on PCL crystallization is partially relaxed by less-rigid confinement, yielding heterogeneous nucleation and subsequent crystal growth along the fastest growth face ((110) plane) perpendicular to the lamellar surface normal. This notion is consistent with the results reported by Ho *et al.*[21] In other words, the c-axis of PLLA crystals in PLLA-*b*-PS was always parallel to the lamellar surface normal in soft confinement, although the lamellar microdomain structure was appreciably distorted.

In summary, the crystal orientation of PCL blocks depends significantly on χ_{PE} when d_{PCL} is smaller (8.3–8.8 nm). That is, we suppose that glassy (or hard) confinement occurs for the crystal orientation observed in E23 with higher χ_{PE}, whereas soft confinement occurs in E07 with lower χ_{PE}. However, crystal orientation is almost independent of χ_{PE} when d_{PCL} is larger (10.4–10.7 nm).

CONCLUSIONS

We have investigated the crystallization behavior and crystal orientation of PCL blocks spatially confined in the PE lamellar morphology with different χ_{PE} and d_{PCL}, where the change in χ_{PE} indicates a change in the rigidity of the confinement space (hard or soft). For this purpose, we controlled χ_{PE} by adjusting the amount of ethyl branches existing in PE blocks during polymerization. When d_{PCL} was smaller and χ_{PE} was higher, the crystallization behavior of PCL blocks was significantly different from that of other copolymers, and the crystal orientation depended on $T_{c,PCL}$; it changed from being randomly oriented to being perpendicular to the PE lamellar surface normal. However, PCL-*b*-PE copolymers with larger d_{PCL} or lower χ_{PE} showed normal crystallization behavior similar to that of crystalline homopolymers without spatial confinement, where the crystal orientation of PCL blocks was parallel to the PE lamellar surface normal irrespective of $T_{c,PCL}$. These results indicate that the PE lamellar morphology with higher χ_{PE} induces hard confinement against PCL crystallization, similar to glassy microdomains, whereas the PE lamellar morphology with lower χ_{PE} provides soft confinement even if d_{PCL} is small. Therefore, the spatial confinement induced by crystallized lamellar morphology is a complex phenomenon that depends on the size and rigidity of the confinement space.

ACKNOWLEDGEMENTS

The one-dimensional SAXS measurements were performed under the approval of Photon Factory Advisory Committee (no. 2010G014).

1 Hamley, I. W. (ed.) *Developments in Block Copolymer Science and Technology* (Wiley, New York, 2004).
2 Nandan, B., Hsu, J. Y. & Chen, H. L. Crystallization behavior of crystalline-amorphous diblock copolymers consisting of a rubbery amorphous block. *J. Macromol. Sci. Part C* **46,** 143–172 (2006).
3 Castillo, R. V. & Müller, A. J. Crystallization and morphology of biodegradable or biostable single and double crystalline block copolymers. *Prog. Polym. Sci.* **34,** 516–560 (2009).
4 Quiram, D. J., Register, R. A., Marchand, G. R. & Ryan, A. J. Dynamics of structure formation and crystallization in asymmetric diblock copolymers. *Macromolecules* **30,** 8338–8343 (1997).
5 Nojima, S., Tanaka, H., Rohadi, A. & Sasaki, S. The effect of glass transition temperature on the crystallization of ε-caprolactone-styrene diblock copolymers. *Polymer* **39,** 1727–1734 (1998).
6 Loo, Y. L., Register, R. A., Ryan, A. J. & Dee, G. T. Polymer crystallization confined in one, two, or three dimensions. *Macromolecules* **34,** 8968–8977 (2001).
7 Huang, P., Zhu, L., Cheng, S. Z. D., Ge, Q., Quirk, R. P., Thomas, E. L., Lotz, B., Hsiao, B. S., Liu, L. & Yeh, F. Crystal orientation changes in two-dimensionally confined nanocylinders in a poly(ethylene oxide)-*b*-polystyrene/polystyrene blend. *Macromolecules* **34,** 6649–6657 (2001).
8 Balsamo, V., Navarro, C. U. & Gil, G. Microphase separation vs crystallization in polystyrene-*b*-polybutadiene-*b*-poly(ε-caprolactone) ABC triblock copolymers. *Macromolecules* **36,** 4507–4514 (2003).
9 Gitsas, A., Floudas, G., Butt, H. J., Pakula, T. & Matyjaszewski, K. Effects of nanoscale confinement and pressure on the dynamics of pODMA-*b*-p*t*BA-*b*-pODMA triblock copolymers. *Macromolecules* **43,** 2453–2462 (2010).

10 Nakagawa, S., Kadena, K., Ishizone, T., Nojima, S., Shimizu, T., Yamaguchi, K. & Nakahama, S. Crystallization behavior and crystal orientation of poly(ε-caprolactone) homopolymers confined in nanocylinders: effects of nanocylinder dimension. *Macromolecules* **45,** 1892–1900 (2012).
11 Loo, Y. L., Register, R. A. & Ryan, A. J. Polymer crystallization in 25-nm spheres. *Phys. Rev. Lett.* **84,** 4120–4123 (2000).
12 Nojima, S., Toei, M., Hara, S., Tanimoto, S. & Sasaki, S. Size dependence of crystallization within spherical microdomain structures. *Polymer* **43,** 4087–4090 (2002).
13 Nojima, S., Kato, K., Yamamoto, S. & Ashida, T. Crystallization of block copolymers. 1. Small-angle X-ray scattering study of an ε-caprolactone-butadiene diblock copolymer. *Macromolecules* **25,** 2237–2242 (1992).
14 Nojima, S., Nakano, H., Takahashi, Y. & Ashida, T. Crystallization of block copolymers: 3. Crystallization behavior of an ε-caprolactone-butadiene diblock copolymer. *Polymer* **35,** 3479–3486 (1994).
15 Ryan, A. J., Hamley, I. W., Bras, W. & Bates, F. S. Structure development in semicrystalline diblock copolymers crystallizing from the ordered melt. *Macromolecules* **28,** 3860–3868 (1995).
16 Sun, Y. S., Chung, T. M., Li, Y. J., Ho, R. M., Ko, B. T., Jeng, U. S. & Lotz, B. Crystalline polymers in nanoscale 1D spatial confinement. *Macromolecules* **39,** 5782–5788 (2006).
17 Sun, Y. S., Chung, T. M., Li, Y. J., Ho, R. M., Ko, B. T. & Jeng, U. S. Crystal orientation within lamellae-forming block copolymers of semicrystalline poly(4-vinylpyridine)-*b*-poly(ε-caprolactone). *Macromolecules* **40,** 6778–6781 (2007).
18 Huang, P., Zhu, L., Guo, Y., Ge, Q., Jing, A. J., Chen, W. Y., Quirk, R. P., Cheng, S. Z. D., Thomas, E. L., Lotz, B., Hsiao, B. S., Avila-Orta, C. A. & Sics, I. Confinement size effect on crystal orientation changes of poly(ethylene oxide) blocks in poly(ethylene oxide)-*b*-polystyrene diblock copolymers. *Macromolecules* **37,** 3689–3698 (2004).
19 Zhu, L., Cheng, S. Z. D., Calhoun, B. H., Ge, Q., Quirk, R. P., Thomas, E. L., Hsiao, B. S., Yeh, F. & Lotz, B. Crystallization temperature-dependent crystal orientation within nanoscale confined lamellae of a self-assembled crystalline-amorphous diblock copolymer. *J. Am. Chem. Soc.* **122,** 5957–5967 (2000).
20 Zhu, L., Calhoun, B. H., Ge, Q., Quirk, R. P., Cheng, S. Z. D., Thomas, E. L., Hsiao, B. S., Yeh, F., Liu, L. & Lotz, B. Initial-stage growth controlled crystal orientations in nanoconfined lamellae of a self-assembled crystalline-amorphous diblock copolymer. *Macromolecules* **34,** 1244–1251 (2001).
21 Ho, R. M., Lin, F. H., Tsai, C. C., Lin, C. C., Ko, B. T., Hsiao, B. S. & Sics, I. Crystallization-induced undulated morphology in polystyrene-*b*-poly(L-lactide) block copolymer. *Macromolecules* **37,** 5985–5994 (2004).
22 Nojima, S., Akutsu, Y., Washino, A. & Tanimoto, S. Morphology of melt-quenched poly(ε-caprolactone)-*block*-polyethylene copolymers. *Polymer* **45,** 7317–7324 (2004).
23 Nojima, S., Akutsu, Y., Akaba, M. & Tanimoto, S. Crystallization behavior of poly(ε-caprolactone) blocks starting from polyethylene lamellar morphology in poly(ε-caprolactone)-*block*-polyethylene copolymers. *Polymer* **46,** 4060–4067 (2005).
24 Sakurai, T., Ohguma, Y. & Nojima, S. Morphological evolution during isothermal crystallization observed in a crystalline-crystalline diblock copolymer. *Polym. J.* **40,** 971–978 (2008).
25 Higa, T., Nagakura, H., Sakurai, T. & Nojima, S. Crystal orientation of poly(ε-caprolactone) blocks confined in crystallized polyethylene lamellar morphology of poly(ε-caprolactone)-*block*-polyethylene copolymers. *Polymer* **51,** 5576–5584 (2010).
26 Sakurai, T. & Nojima, S. Significant increase in the melting temperature of poly(ε-caprolactone) blocks confined in the crystallized lamellar morphology of poly(ε-caprolactone)-*block*-polyethylene copolymers. *Polym. J* **43,** 370–377 (2011).
27 Halasa, A. F., Lohr, D. F. & Hall, J. E. Anionic polymerization to high vinyl polybutadiene. *J. Polym. Sci* **19,** 1357–1360 (1981).
28 Bywater, S., Mackerron, D. H., Worsfold, D. J. & Schue, F. The anionic polymerization of butadiene in the presence of dipiperidinoethane. *J. Polym. Sci* **23,** 1997–2003 (1985).
29 Brandup, J. & Immergut, E. H. *Polymer handbook 3rd edn* (Wiley, New York, 1989).
30 Crescenzi, V., Manzini, G., Calzolari, G. & Borri, C. Thermodynamics of fusion of poly-β-propiolactone and poly-ε-caprolactone. Comparative analysis of the melting of aliphatic polylactone and polyester chains. *Eur. Polym. J* **8,** 449–463 (1972).
31 Nojima, S., Tsutsui, H., Urushihara, M., Kosaka, W., Kato, N. & Ashida, T. A dynamic study of crystallization of poly(ε-caprolactone) and poly(ε-caprolactone)/poly(vinyl chloride) blend. *Polym. J.* **18,** 451–461 (1986).
32 Miyazaki, T., Hoshiko, A., Akasaka, M., Sakai, M., Takeda, Y. & Sakurai, S. Structure model of a poly(vinyl alcohol) film uniaxially stretched in water and the role of crystallites on the stress-strain relationship. *Macromolecules* **40,** 8277–8284 (2007).
33 Sakamoto, N. & Hashimoto, T. Order-disorder transition of low molecular weight polystyrene-*block*-polyisoprene. 1. SAXS analysis of two characteristic temperatures. *Macromolecules* **28,** 6825–6834 (1995).
34 Avrami, M. Kinetics of phase change. I. General theory. *J. Chem. Phys.* **7,** 1103–1112 (1939).
35 Avrami, M. Kinetics of phase change. II. Transformation-time relations for random distribution of nuclei. *J. Chem. Phys* **8,** 212–224 (1940).
36 Takeshita, H., Gao, Y. J., Takata, Y., Takenaka, K., Shiomi, T. & Wu, C. Formation of phase structure and crystallization behavior from disordered melt for ethylene-isoprene block copolymers and their blends. *Polymer* **51,** 799–806 (2010).
37 Castillo, R. V., Müller, A. J., Raquez, J. M. & Dubois, P. Crystallization kinetics and morphology of biodegradable double crystalline PLLA-*b*-PCL diblock copolymers. *Macromolecules* **43,** 4149–4160 (2010).
38 Yoo, E. S. & Im, S. S. Effect of molecular orientation on the biodegradability of aliphatic polyester. *Macromol. Symp.* **142,** 13–21 (1999).